Materials and Design, Volume 121, 5 May 2017, Pages 51–60
DOI: 10.1016/j.matdes.2017.02.054

Study on strengthening mechanism of Ti/Cu electron beam welding

Shun Guo[a], Qi Zhou[a,*], Yong Peng[a,*], Xiangfang Xu [b], Chenglei Diao [b], Jian Kong[a] , TianYuan Luo[a], KeHong Wang[a], Jun Zhu[c]

[a] School of Materials Science and Engineering, Nanjing University of Science and Technology, 210094, Nanjing, China

[b] Welding Engineering and Laser Processing Centre, Cranfield University, Bedford, MK43 0AL, UK

[c] Nanjing Institute of Technology, 210094, Nanjing, China

*Correspondence author: Tel: +86 025-84315776;

E-mail: cheezhou@njust.edu.cn (Q. Zhou), ypeng@njust.edu.cn (Y. Peng)

Abstract: Welding-brazing method is widely used for dissimilar metals welding. However, it is becoming increasingly difficult to further improve the connection strength by controlling the formation of the transition layer. In this study, an innovative welding method referred to as adjacent welding was addressed, which greatly improved the tensile strength of Ti/Cu dissimilar joint. The strength of new joint could reach up to 89% that of copper base metal, compared to the use of a traditional welding-brazing method which strength coefficient is within the limit of 70%. In order to determine the strengthening mechanism of adjacent welding, optical microscopy, SEM, EDS and XRD were applied for the analysis of microstructure and phase structure. Furthermore, tensile strength was also tested. The results show that due to the process of remelting and reverse solidification of intermetallic compounds (IMCs) layer, a less complex and thinner IMCs layer was formed and TiCu (553HV) with high embrittlement existing in the front of titanium substrate was changed into Ti_2Cu (442HV). Performances of joints were optimized by these changes. An interpretation module was presented for the mechanism.

Keywords: welding-brazing, adjacent welding, dissimilar welding joints, intermetallic compounds.

1. Introduction

Dissimilar metals welding is an important technology in the modern industry. It is characterized by the ability to maximize the use of a variety of advantages of materials for industrial production [1-5]. The effective connection of Ti/Cu dissimilar materials not only meets the requirements of thermal conductivity, electrical

conductivity, corrosion resistance and wear resistance, but also meets the requirements of high strength but light weight. Therefore, it will have broad application prospects in the fields of aerospace, instrumentation, electronics, chemical industry and so on [6]. In addition, selected as the transition layer material for dissimilar metals welding, Cu and its alloys also present some attractive advantages [7-12], so successful connection of Ti/Cu would give one more option to achieve the welding of titanium and other metals using copper as the transition layer material.

Comparing the thermo-physical properties of titanium and copper in Tab.2, it shows that there are some significant differences between each other. In the aspect of compatibility of the two materials, fusion welding joint of titanium and copper exhibits inferior mechanical properties due to the formation of brittle intermetallic phases Ti_xCu_y and eutectic compounds with low melting point. Meanwhile, titanium and copper could be easily oxidized at high temperatures due to strong activity, and they are capable of strong absorption of nitrogen and hydrogen, which will cause brittle fracture. Given the reason above, the welding of titanium and copper is mainly focused on brazing [13] and solid phase welding at present, such as friction welding [14-15], explosive welding [16-17] and collision welding [18]. Previous research results indicate that the method of solid phase welding exhibits certain advantages due to its perfect connection and good welding quality.

Aydın [19] reported the bonding of Ti-6Al-4V and Cu was successfully achieved by diffusion method with suitable welding parameters. Diffusion transition zone near the interface consisted of various phases such as βCu_4Ti, Cu_2Ti, Cu_3Ti_2, Cu_4Ti_3 and CuTi. The maximum shear strength was found to be 2.171 kN. Yao [20] investigated the bonding ability of Ti/Cu by friction stir welding and the results showed that the defect-free lap weld with the well-formed surface was obtained when rotation speed and travel speed were 800 r/min and 400 mm/min respectively. A maximum failure load reached 95% of T2 copper strength and fracture occurred at the advancing side of copper with a typical ductile character. These studies showed the feasibility of solid phase welding. However, there are some insurmountable limitations in the application of solid phase connection, such as weight gain of superposition, limited joint form and low usage temperature. Therefore, it is quite essential to further study fusion welding which can provide a more reliable and higher strength of Ti / Cu joint.

Electron beam welding (EBW), with high energy density, large depth to width ratio, and cutting off the adverse effects of air under vacuum [3, 21], is of high interest for the welding of dissimilar materials. Liu [22] reported that using non-centered electron beam for the welding of QCr0.8 and TC4, the maximum value of tensile strength was 270.5 Mpa, equivalent to 75% that of QCr0.8. But at the interface of titanium and copper, the existence of some unfavorable intermetallic compounds (IMCs) such as TiCu and Ti_3Cu, resulted in the weakening of joint. Based on this study, Chen [23] presented a novel method referred to as electron beam superposition welding which was intermetallic layer produced by centered welding was fragmented and remelted during Cu-side non-centered welding. The strength coefficient of Ti/Cu joint was improved by a small amount to 77%. However, no significant changes of phase

construction had occurred at the interface and joint strength was still greatly limited by the intermetallic layer.

To summarize, many previous studies [6,19,31] state that there is a bottleneck to further improve the performance of Ti/Cu joint. So, the aim of this study was to explore an ideal method of EBW to further optimize the Ti/Cu fusion welding joint. A new improved approach named as electron beam adjacent welding was proposed for the first time. An excellent phase structure and distribution of IMCs layer, as well as a high strength joint, were obtained. Microstructural and mechanical properties, distribution, and evolution of IMCs layer in the weld were investigated.

2. Experimental procedure

2.1 Materials

Ti-6Al-4V and T2 copper (GB/T 2059-2008) plates were used as EBW materials with the dimension of 100×50×4 mm and no groove. Chemical compositions and mechanical properties are listed in Table 1. All specimens were prepared carefully by fine polishing with sandpapers of various grit sizes (240#, 400# and 600#) and surface cleaning with absolute alcohol before welding. Specimens were firmly fixed in the form of butt joint.

Table 1

Chemical compositions (wt.%) and Mechanical properties of the materials.

Materials	Elements (wt. %)					Hv	δ	Rm / MPa
Copper (T2)	Cu + Ag	O	Fe	S	Ni	70-90	⩾20	236
	99.9	0.06	0.005	0.005	0.005			
Ti-6Al-4V	Ti	Al	V	Fe	C	310-330	⩾10	895
	89.12	6.42	4.30	0.05	0.03			

Table 2

Thermo-physical properties of titanium and copper

Materials	Crystal lattice	Density $kg \cdot m^{-3}$	Specific heat $J \cdot kg^{-1} \cdot K^{-1}$	Melting point K	Fusion heat $kJ \cdot mol^{-1}$	Thermal conductivity $W \cdot m^{-1} \cdot K^{-1}$	Expansion coefficient $1E\text{-}6 \cdot K^{-1}$
Titanium	hcp	4540	544.2	1943	15.45	15.7	7.14
Copper	fcc	8960	380.9	1357	13.26	393.6	16.4

2.2 Welding methods

Lots of previous studies [3,4,22,23] have shown that non-centered welding was useful for dissimilar metals welding but needed to be further optimized. Therefore, a new improved method of adjacent welding was used in this paper. Schematic diagram of the welding process and transverse sections of weld were shown in Fig.1 and 2 respectively. Adjacent welding means another welding occurs close to former weld at the front or back side after taking welding-brazing at first. There is no cross between

two welds. The advantage is that during adjacent welding, phase transition would be generated in the IMCs layer of welding-brazing joint, which is useful to improve strength.

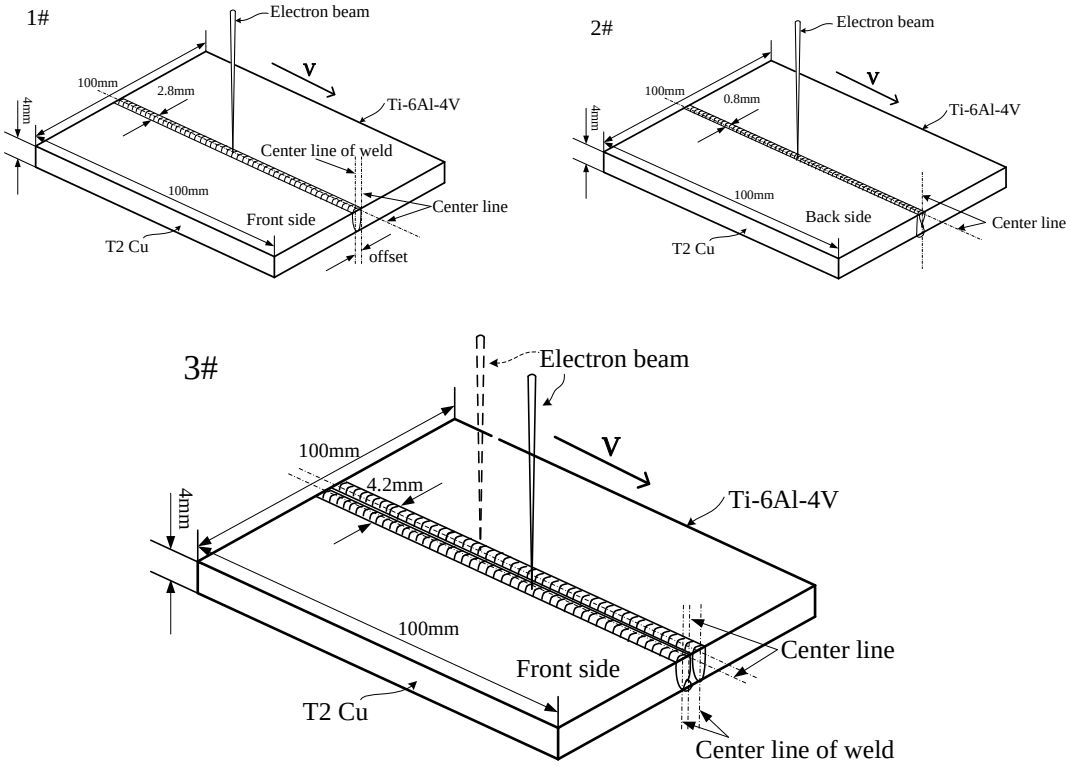

Fig.1 Schematic diagram of welding process with adjacent welding of front side: 1# non-centered welding (welding-brazing), 2# root welding, 3# adjacent welding. Detailed welding parameters are shown in Tab.3.

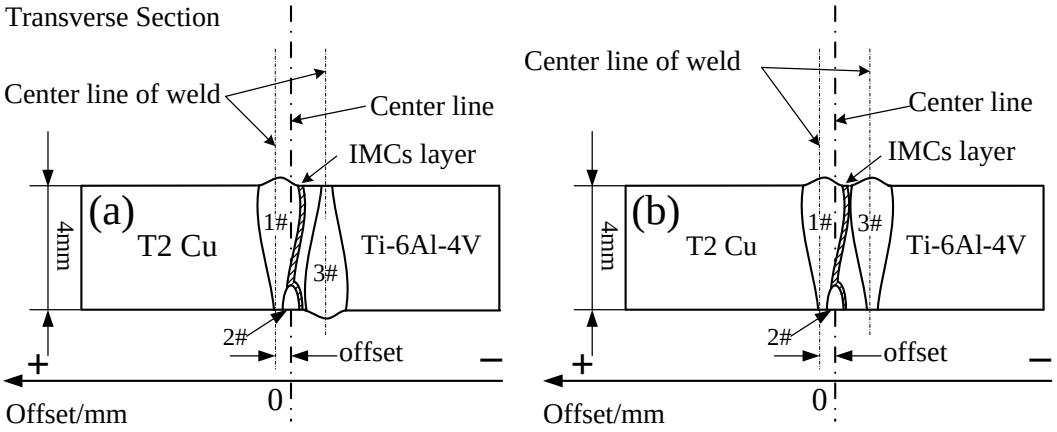

Fig.2 Two types of transverse sections of weld seam due to different welding direction: positive offset means beam is focused on copper plate and negative offset means beam is focused on titanium plate.

There are two types of transverse sections of weld seam due to different welding direction, but many experiments indicated that the effect of welding direction is not

significant. Due to the characteristics of deep and narrow weld of EBW, quality of weld root was poor [3,24,25]. To improve the root strength, small power root welding was added in the paper.

Table 3
The optimization of the operating and geometrical welding parameters.

parameters	Cu-side EBW		Cu-side EBW + adjacent welding			Ti-side EBW		Ti-side EBW + adjacent welding		
	1 #	2#	1#	2#	3#	1#	2#	1#	2#	3#
Voltage (kV)	60	60	60	60	60	60	60	60	60	60
Filament current (mA)	432	428	430	430	428	430	425	431	425	425
Focus current (mA)	670	670	670	670	670	672	672	670	670	670
Gun vacuum (E-3pa)	3.4	4.5	3.2	3.6	3.6	6.2	6.8	5.8	6.5	7.0
Chamber vacuum (E-2pa)	6.6	6.2	6.3	6.8	6.5	5.3	4.6	5.7	4.9	6.2
Work distance (mm)	294	294	294	296	295	294	295	294	295	295
Welding speed(mm/s)	10	15	10	15	10	10	15	10	15	10
Beam current (mA)	45	20	45	20	25	25	20	25	20	45
Offset(mm)	+1.4	0	+1.4	-0.8	0	-0.3	0	-0.3	-0	+1.2

2.3 Characterization methods

A Zeiss optical microscope and a Quant 250FEG scanning electron microscope (SEM) equipped with an energy-dispersive X-ray spectrometry (EDS) system were applied for the observation of microstructure and chemical composition of samples. All samples cut off from weld with the dimension of 10×5×4mm were prepared with standard grinding, polishing, and corrosion before observation. Fractional corrosion method was used. Etching solution for copper and titanium were 10g $FeCl_3$ + 10ml HCl + 30ml H_2O and kroll reagent consisting of 1vol.% HF, 6vol.% HNO_3 and 93vol.% H_2O for 10s, respectively. The intermetallic phase structures at the interface of weld were detected by a Bruker-AXS D8 Advance X-ray diffractometer (XRD) with the scanning range of 20-100°(2θ) and step size of 0.02°.

To investigate the mechanical properties of Ti/Cu electron beam welding joints, UTS of joint was evaluated by a tensile testing machine (maximum tensile strength 10 kN) with the speed of 3 mm/min at room temperature. Three tensile samples of each kind of joints were tested and the average value was recorded. Standard dimension of samples was according to GB/T228-2002.

3. Results and discussion

3.1 Bonding characteristics

Binary equilibrium diagram of titanium and copper was presented in Fig.3, which is a finite solid solution and eutectic transition state diagram. It reveals that solid solubility of Cu in Ti (α, β phase), Ti in Cu (Cu phase) are quite limited. But there are a wide range of compounds that may be formed including phases of Ti_2Cu, TiCu,

Ti_3Cu_4, Ti_2Cu_3, $TiCu_2$, $\beta TiCu_4$ and a variety of low melting point eutectic such as $\alpha/\beta Ti+Ti_2Cu$ (790°C/1005°C), $Ti_2Cu+TiCu$ (960°C), $TiCu_2+TiCu_3$ (875°C). Phases of TiCu (533HV), Ti_3Cu_4 (500HV), Ti_2Cu_3 (597HV), $TiCu_4$ (504HV) possess a high hardness. Existence of these compounds and eutectic are detrimental to the joint and failure occurs often due to the adverse growth of these intermetallic compounds and low melting point eutectic [6,16,19,22]. The cooling of EBW is a non-equilibrium solidification process, it is difficult for peritectic reaction to take place in the weld. Phase diagram analyses are consistent with previous research results [6,9,13,26].

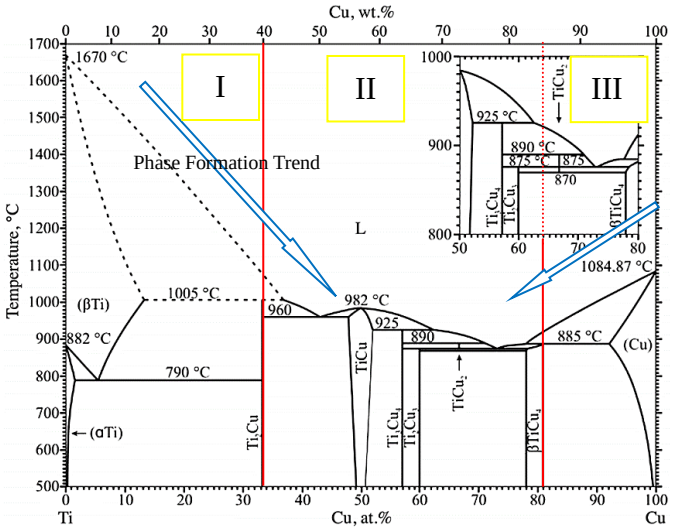

Fig.3 Binary equilibrium diagram of Ti/Cu

3.2 Characteristic of joint

3.2.1 Ultimate tensile strength (UTS)

UTS which results are presented in Fig.4, was selected to evaluate the effect of different process on Ti/Cu electron beam welding. Fig.4a indicates the strength values of copper side welding-brazing and Fig.4b indicates the values of titanium side adjacent welding after carrying out copper side welding-brazing with offset of 1.4mm. Correspondingly, Fig.4c shows the values of titanium side welding-brazing. And Fig.4d shows the values of copper side adjacent welding after carrying out titanium side welding-brazing with an offset of -0.3mm.

Fig.4a shows that Ti/Cu EBW with a positive offset on copper side has an obvious trend of first increase and then decrease. The curve is consistent with former welding-brazing studies [2,3,19,27]. There is a reasonable window for the offset. Too large offset resulting in an invalid atomic diffusion or too small offset leading to an overgrowth of intermetallic compounds will be negative on strength. Fig.4c shows that when offset value becomes negative and electron beam is completely biased towards titanium side, it becomes almost impossible to weld.

However, after taking the welding-brazing procedure at first with suitable offset, another procedure referred to as adjacent welding was added. The strength of Ti/Cu joints gets a great improvement which strength even reaches up to 89% that of copper

base metal. Chen [23] reported an optimized electron beam superposition welding and strength coefficient was 76.7%, which was hard to improve due to complex IMCs. The UTS of adjacent welding joints were shown in Fig.4b, d, compared to Fig.4a c, it could be indicated that adjacent welding is beneficial to connect Ti and Cu.

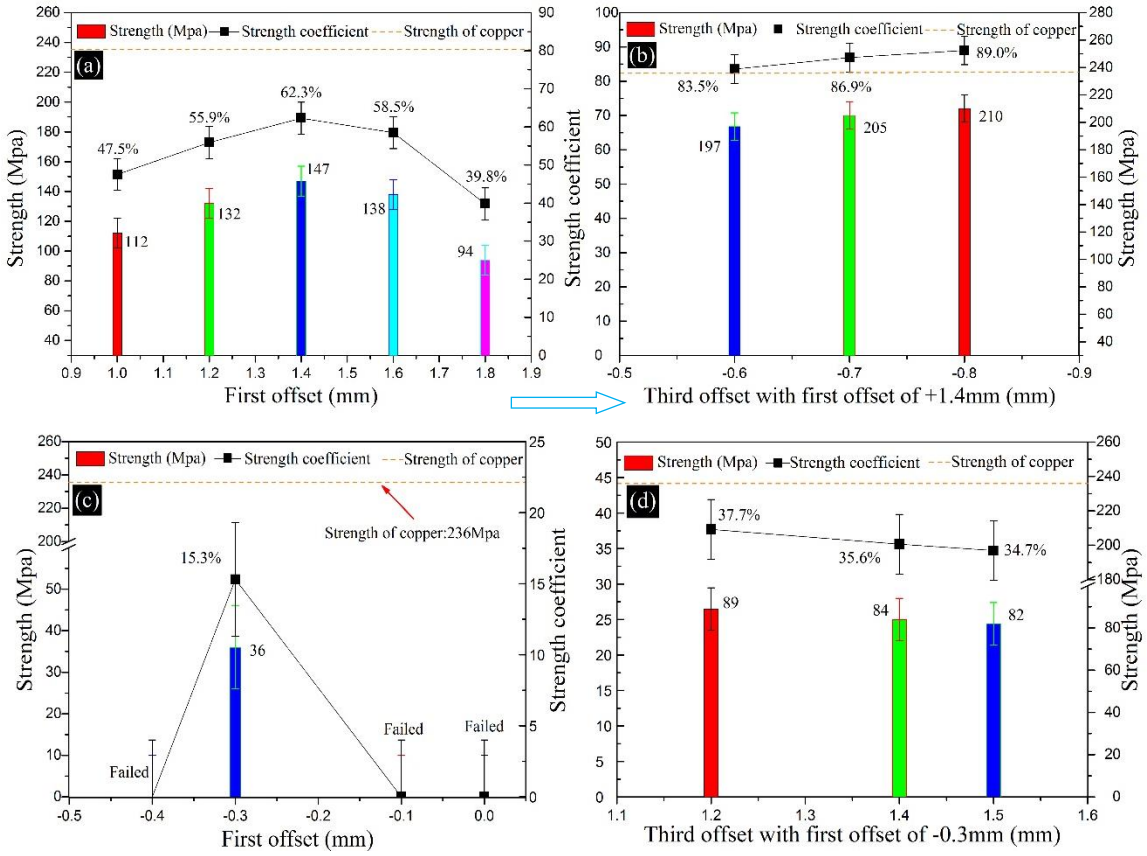

Fig.4 Results of UTS of Ti/Cu electron beam welding. (a): Electron beam brazing-welding(EBBW) with different offset on copper side; (b): EBBW with the offset of +1.4mm on copper side and then adjacent welding with different offset on titanium side; (c): EBBW with different offset on titanium side; (d): EBBW with the offset of -0.3mm on titanium side and then adjacent welding with different offset on copper side.

In addition, by contrasting Fig4.a and d, although the parameters of EBW on copper side were similar, there is a major strength decrease and copper side welding-brazing has an obvious advantage against copper side adjacent welding. The reason of the result is due to the increase of titanium content in the weld after carrying out titanium side welding-brazing at first for adjacent welding procedure. Excessive titanium content in the weld makes IMCs become more complicated and uncontrollable. Wang [26] reported that the welding of Ti alloy and 304 stainless steel was not feasible due to lots of brittle, continuously distributed Ti-Fe intermetallic and optimization by using copper filler metal to connect Ti alloy and steel also presented a problem of weak Ti/Cu interface. Shen [29] investigated the properties of Ti/Cu joints with silver interlayer by diffusion bonding and demonstrated that fracture initiation and propagation occurred at the Ag/OFC interface and this interface was the weak point because of the unfavorable formation of complex Ti-Cu compounds. Tashi [30] reported vacuum brazing of Ti-6Al-4V and stainless steel using AgCuZn filler metal

and stated that by increasing the brazing temperature various intermetallic compounds which were mainly a combination of CuTi and Fe-Cu-Ti were formed and these IMCs largely lowered the strength. These studies reveal that it is great important to control the formation of Ti-Cu compounds.

3.2.2 Microstructural examination

From Tab.3, it can be seen there are four kinds of joints, but Fig.4 shows that tensile strength of titanium side welding-brazing and copper side adjacent welding was not satisfactory. Therefore, in this paper, microstructural examination was focused on the comparative analysis of copper side welding-brazing and titanium side adjacent welding. SEM pictures of welding-brazing and adjacent welding were shown in Fig.5.

Fig.5a shows a low magnification picture of adjacent welding and indicates that there is a small piece of unmelted titanium interlayer left behind between two welds and IMCs layer of the welding-brazing joint was not destroyed by this innovative process. Fig.5b and b' present the weld section surface of adjacent welding and there are four areas classified into weld zone, bright zone (FS zone), IMCs layer and titanium interlayer. Regarding to the bright zone, it could be known that it is final solidification (FS) zone. The reason is that the weld dendrite direction is not perpendicular to FS zone according to Fig.5b'. Besides, a bright interlayer which is a branch of FS zone and noted by a red arrow existed between two dendrites in the weld zone.

The thermal conductivity of copper (393.6 $W \cdot m^{-1} \cdot K^{-1}$) is much greater than that of titanium (15.7 $W \cdot m^{-1} \cdot K^{-1}$), so it would be very easy to dissipate heat along the copper side and dendrite growth extended rapidly to almost whole weld during cooling and then weld zone was formed. On the contrary, it was quite slow for the dendrite growing at titanium side. The width of dendrite zone in Fig.5c is about 25.5μm. Dezellus [28] reported a similar Ti_xCu_y reaction layer with a thickness of 15-25μm at titanium interface. The small dendrite zone is the IMCs layer. At the final stage of cooling, due to limitation of concentration gradient at the forefront of liquid phase and different orientations of the two dendrites, the final solidification (FS) zone was formed and held between weld zone and IMCs layer.

Asymmetric dendrite growth is common in dissimilar metals welding due to offset and thermal conductivity [2,3]. Chen [23] reported electron-beam superposition welding on IMCs layer of Ti/Cu and the weld microstructures for Cu-side non-centered welding was similar with Fig.5b. Cao [31] studied on the cold metal transfer Ti/Cu welding-brazing and the weld microstructure was composed of Cu-Cu welding joint and Cu-Ti brazing joint, IMCs layer was also in a small scale.

Fig.5c, e respectively show the weld morphologies of welding-brazing and adjacent welding, from which it can be known IMCs layer was changed obviously after adjacent welding. Dendrite structure was reshaped at the temperature field of adjacent welding. Fig.5c indicates that at titanium side, dendrite growth of welding-brazing was based on titanium substrate and proceeded toward the center of molten pool and the dendrite terminals are clear and uneven. The width of IMCs layer is 25.5μm and it

accounts for 65% of total width of IMCs layer and FS zone. But after carrying out adjacent welding, former dendrite terminals were changed into a new interface and dendrite attached to this interface grew up again shown in Fig.5d. Width and proportion are dropped to 20.4μm and 50% respectively.

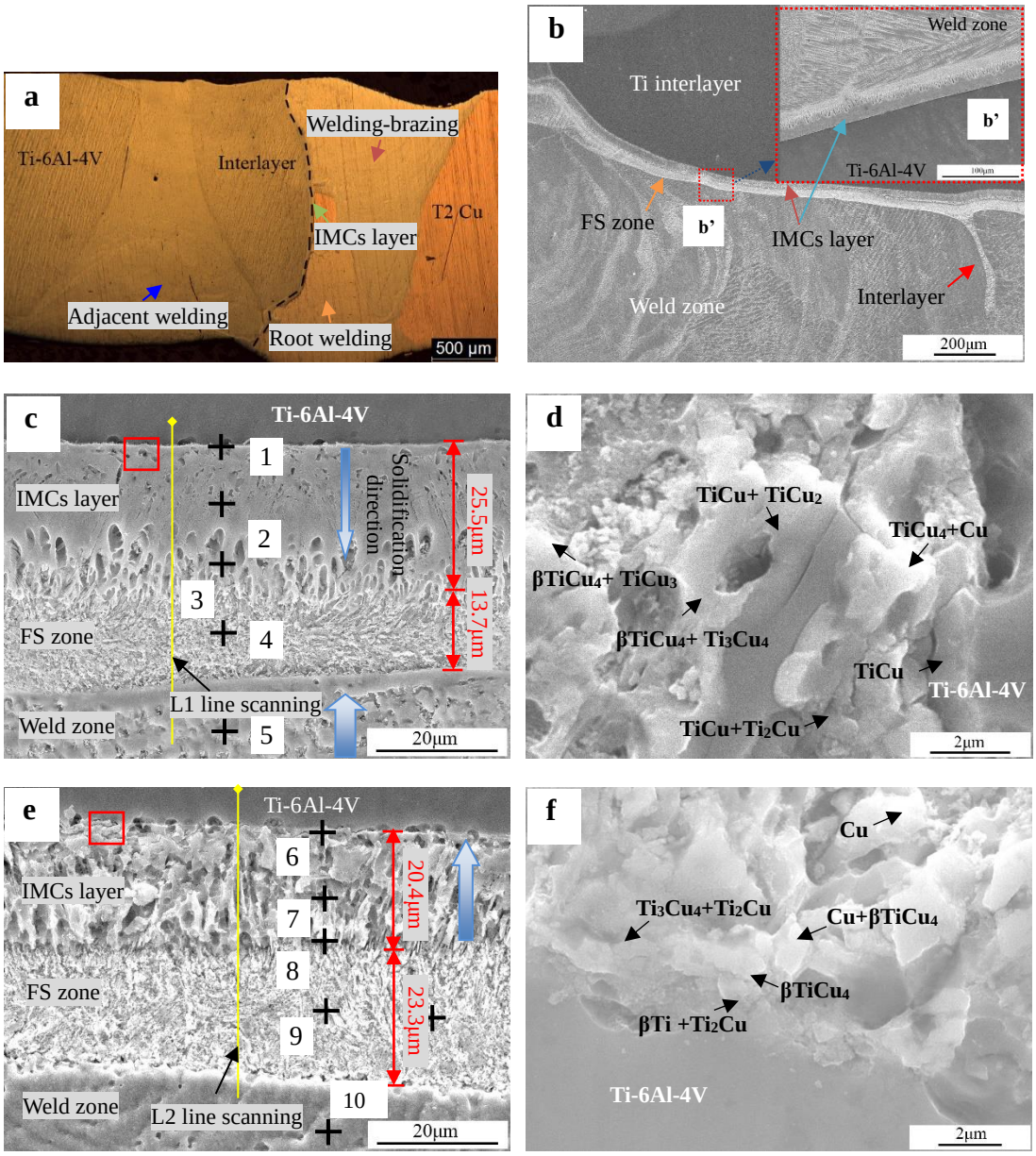

Fig.5 Microstructural diagram of welding-brazing joint and adjacent welding. (a): microstructure of adjacent welding; (b): molten pool ; (c) IMCs layer of welding-brazing joint; (d) IMCs layer of adjacent welding joint. (e) magnification in red outline of c; (f) magnification in red outline of e.

Fig.6 shows the line scanning results which sampling position is indicated by the yellow line in Fig.5c, e. It shows due to the technology characteristic of welding-brazing process, titanium content melt into molten pool was small. The diffusion distance of titanium is about 23μm and it becomes shorter (14μm) after adjacent welding. there is also a concentration gradient for copper which is increasing but decreasing for titanium. Fig.7 shows more accurate results of Ti and Cu elements distribution by scanning the points marked in Fig.5. It demonstrates the change of

concentration gradient and also shows the range of Ti-Cu intermetallics is narrow and IMCs are mainly gathered near the titanium interface. In addition, copper content of welding-brazing joint is higher than that of adjacent welding joint in IMCs layer, but the conclusion is opposite for titanium by comparing Fig.7a, b.

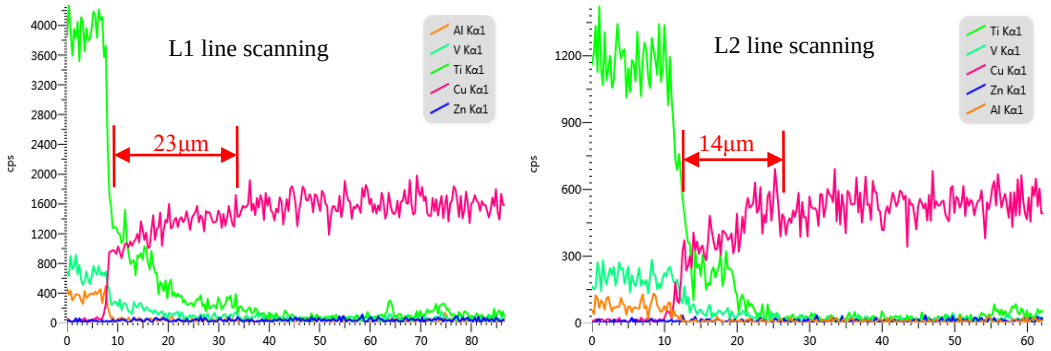

Fig.6 Line scanning results of the yellow lines shown in Fig.5

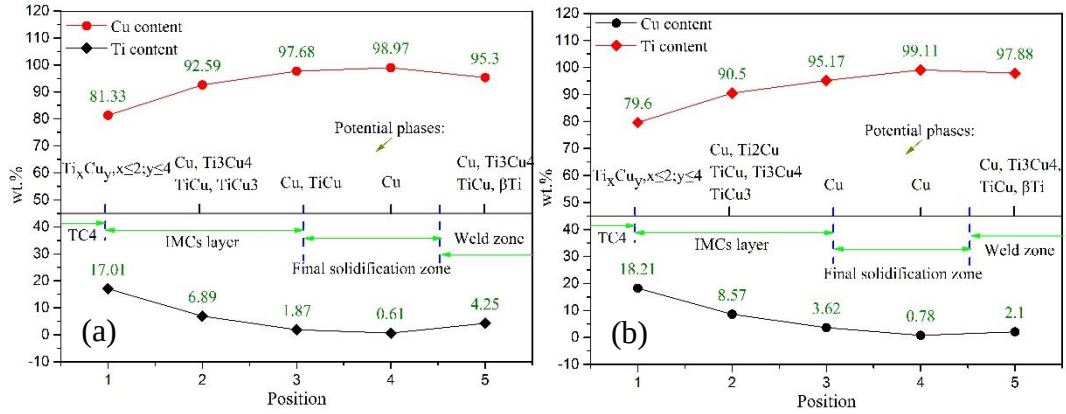

Fig.7 EDS results of the points marked in Fig. 5. (a) welding-brazing, (b)adjacent welding

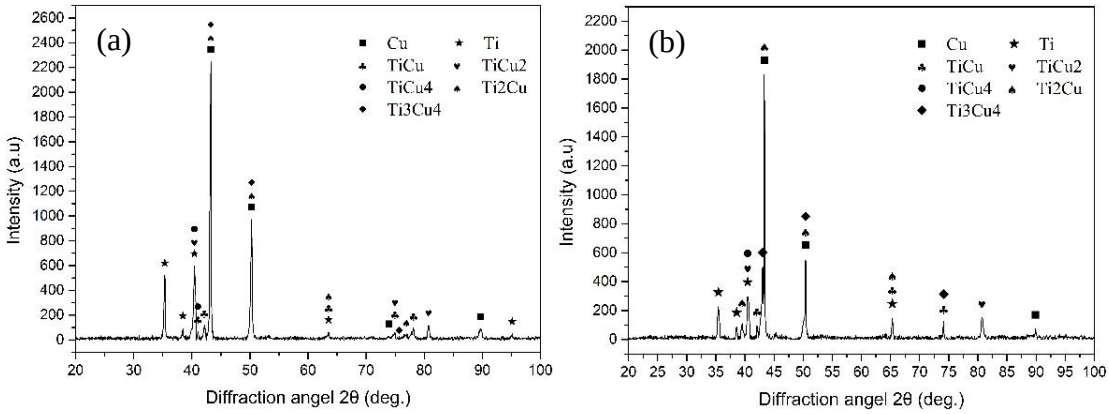

Fig.8 XRD results of the welds of welding-brazing (a) and adjacent welding (b)

XRD was also used to clarify the phase of weld and its results was shown in Fig.8. Its results state that there are many intermetallics of low relative content existing in the weld, including TiCu, $TiCu_2$, $TiCu_4$, Ti_2Cu, Ti_3Cu_4. These phases present a feature of low formation enthalpy and can be separated from liquid phase directly or by eutectic reaction in cooling, that is competitive in the process of non-equilibrium solidification of welding. Fig.8 also shows that the two strongest characteristic peaks of TiCu (41.11°, 42.34°) weaken but the main peak of Ti_2Cu (39.49°) gets strengthen after

adjacent welding. There is a little deviation from the theoretical value for the peak position of these phases due to the residual stress caused by the rapid cooling.

Fig.5d, f show higher magnification pictures of the red outline in titanium interface of Fig.5c, e. Potential phases are marked out at different luminance regions by combining EDS and XRD. The phase distribution demonstrate that titanium element melt into molten pool was small and the range of Ti-Cu intermetallics is narrow and it gets narrower after adjacent welding. Adjacent welding tends to remove titanium element from molten pool. Furthermore, Fig.5d presents a more complicate phase distribution and a larger space scale of Ti-Cu intermetallics. The phase closest to titanium interface was changed from TiCu into Ti_2Cu. These results also illustrate that there were a remelting and crystallization in IMCs layer, which would have a positive effect on joint during adjacent welding procedure.

As a summary of foregoing, reshaped morphology and element redistribution after adjacent welding would account for the joint strengthening. Additionally, in rapid solidification of welding-brazing, a problem of large residual stress would be existed in the weld resulting in reduction of joint strength. Chu [9] investigated the joining of CP-Ti/Q345 sheets by Cu-based filler metal and inferred mechanical properties of the joint were restricted by the Ti-Cu intermetallics and residual stress. Improving the filler metal to control the IMCs is a feasible way to overcome the difficulty. Bokstein [32] studied the formation kinetics of Ti-Cu system and indicated the thermodynamic forces, such as the stress gradient $\nabla\sigma$, is one of considerations reasonably accounting for formation of IMCs. Accordingly, the residual stress should be taken into account for the joint strength. During adjacent welding, former IMCs layer of welding-brazing which was the weakest in the weld was remelted and the stress was released. In the next cooling process, a new phase distribution with a less complex and thinner IMCs layer was formed, so the stress state got optimized. And also the adjacent welding played a role seeming like local heat treatment due to its welding position and further optimized the stress state.

3.3 Strengthening mechanism

3.3.1 Microstructure evolution

As what is concluded from the above, adjacent welding would lead to the remelting of IMCs layer of welding-brazing. The reason is that IMCs layer was so close to the adjacent welding molten pool which boundary temperature was about the melting point of titanium (1670℃), therefore, at the temperature field of adjacent welding, the temperature of IMCs layer would exceed the melting point of Ti-Cu intermetallics and then lead them to remelt. But due to the high thermal conductivity (393.6 $W \cdot m^{-1} \cdot K^{-1}$) of copper in the FS zone and weld, the remelting was prevented. The content of Ti/Cu and microstructures of two kinds of welds at FS zone are almost the same, which proves the remelting was blocked and only occurred in the IMCs layer.

During the cooling of adjacent welding, heat dissipation of IMCs layer was changed and new solidification would be going on according to the direction indicated by the

blue arrow in Fig.5e, which was contrary to Fig.5c. Therefore, a new IMCs layer was formed, which dendrite growth was based on the solid interface of FS zone. New phase formation would be in accordance with the trend line in area III of Fig.3. This area is a removal process of titanium element, so titanium atoms were gradually enriched at the front of solid-liquid interface, which led to previous diffused titanium atoms being pushed back and improved the phase formation of Ti_2Cu. The diffusion distance of titanium decreased to 14μm from 23μm after adjacent welding.

3.3.2 Model for interpretation

Schematic presentations of welding reaction of welding-brazing and adjacent welding were shown in Fig.9, 10. These two procedures were divided into four basic steps according to the interface morphologies of IMCs layer, respectively. After applying the welding-brazing method for Ti/Cu dissimilar connection, the strength of joint could reach about 70% that of copper substrate. Its process was summarized as follows:

(i). Fig.9a shows that during the process of welding-brazing, substrates of copper and titanium were melt into molten pool, but the main component of the pool was filled with copper due to positive offset, and there was an enrichment zone of titanium at the front of titanium substrate.

(ii). Fig.9b is the initial structure of weld seam as it cooled. At the front of titanium substrate, due to favorable nucleation condition and small formation enthalpy of Ti_2Cu, TiCu, these phases were formed by the eutectic reaction at 960°C and precipitation at 982°C, respectively. On the other side of molten pool, copper element attached to copper substrate formed nuclear and grew up at 1084°C.

(iii). Fig9.c shows that caused by different thermal conductivity, the dendrite at copper side grew up rapidly and extended quickly to almost the whole weld zone. However, at titanium side, due to the concentration gradient and limited content of titanium, phase formation trend was gradually changed from area I to III in Fig.3, the IMCs could not grow continuously. Corresponding to the content of titanium, $TiCu_2$, $TiCu_3$ were sequentially formed, and finally the copper dendrite began to be formed and grow up due to the lack of titanium atoms, but the growth speed was slow because of poor heat dispersion velocity at titanium side.

(iv). At the last stage of cooling process shown in Fig.9d, dendrite zone of two sides met. Due to their different microstructure and orientation, a liquid phase of final solidification would be held between each other and when it completely cooled down, the final solidification (FS) zone was formed. Meanwhile, because of the consumption of titanium element in the formation process of IMCs and dendrite growth, there was almost no titanium element in FS zone according to the EDS results of Fig.7. In addition, an unsatisfied stress state would be existed in the weld due to the

rapid cooling process.

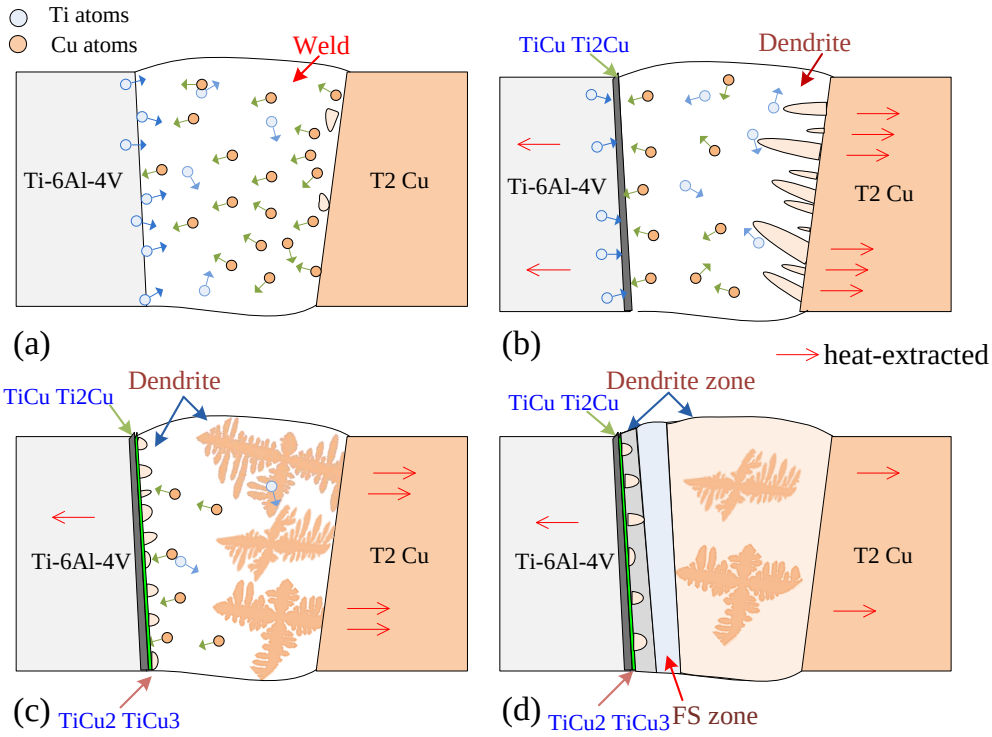

Fig.9 Schematic presentations of welding reaction of welding-brazing

In the whole process of cooling, as the heat dispersion velocity at titanium side was very slow, the complex and brittle IMCs layer got effectively grown, which led to the failure of continuity of the ductile substrate and a poor stress state. Thus, it was difficult to further improve the strength of joint. To eliminate the harmful effect of IMCs layer, adjacent welding was utilized, which process was summarized as follows:

(i). Fig.10a shows the microstructure of welding-brazing joint after cooling. As discussed above, due to the small heat dispersion velocity at titanium side, complicated and excessive IMCs were formed at the front of titanium interface. According to the concentration gradient and formation enthalpy, the formation of new phase was based on the sequence as TiCu, Ti_2Cu, Ti_3Cu_4, $TiCu_2$, and finally the copper dendrite began to grow up.

(ii). Adjacent welding arose near former welding-brazing seam at titanium side. As the melting point of IMCs was low (about 1000°C) and close to the molten pool, remelting of IMCs layer occurred. However, due to high thermal conductivity (393.6 $W \cdot m^{-1} \cdot K^{-1}$) of copper in the FS zone and weld zone, the remelting was prevented and only occurred in IMCs layer shown in Fig.10b.

(iii).After the heat source leaving, the remelting zone began to cool down and crystallization occurred immediately. Due to the characteristics of liquid concentration, new phases were going to be formed on the basis of the phase formation trend of area III in Fig.3. Copper dendrite attached to the solid interface of FS zone would form the nuclear and grow up first. As the phase

formation trend is a removal process of titanium element, titanium atoms were gradually enriched at the front of solid-liquid interface shown in Fig.10c.

(iv). Because of the high heat dispersion velocity at copper side, copper dendrite grew up quickly resulting in lots of titanium atoms being pushed back to the front of titanium interface. Therefore, at the end of solidification, new phases would be formed according to the phase formation trend of area I in Fig.3, which improves the formation of Ti_2Cu phase. Due to the reduction of diffusion distance of titanium element, a less complex and thinner IMCs layer was formed shown in Fig.10d. Accordingly, stress state was improved.

As a result, in the process of remelting and reverse solidification of IMCs layer, the microstructure and stress state got a beneficial improvement and the strength of joints reached 90% that of copper substrate.

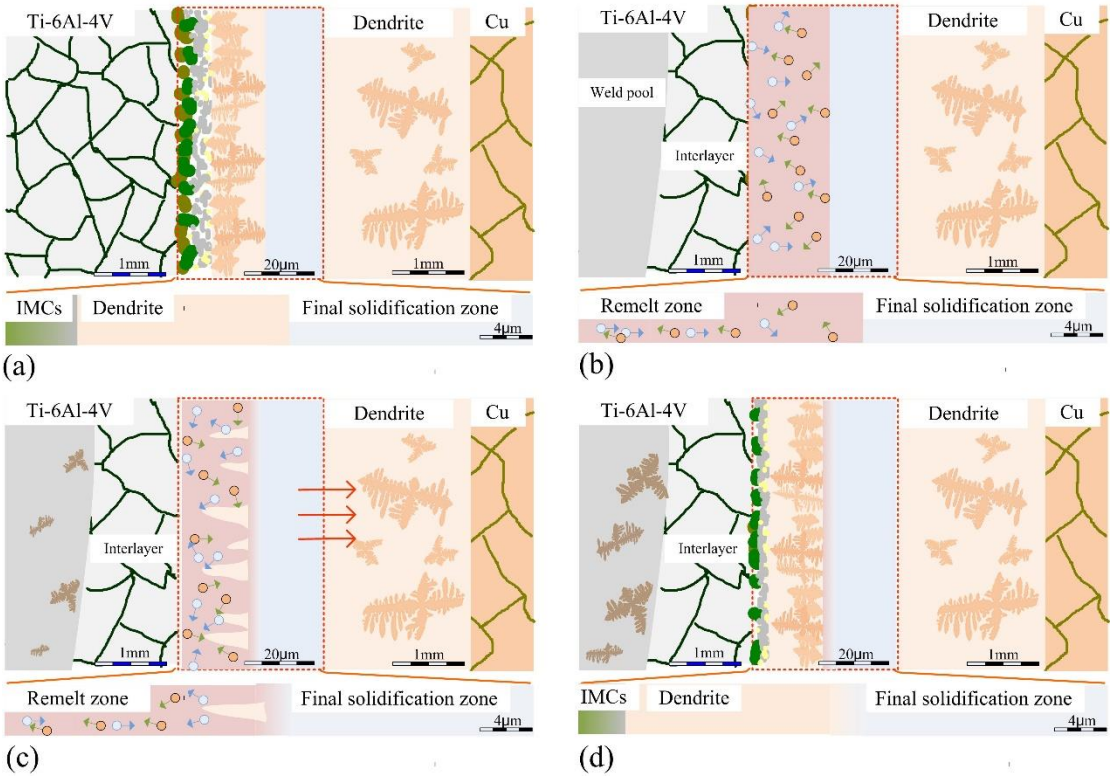

Fig.10 Schematic presentations of welding reaction of adjacent welding

3.4 Fracture and failure

The fracture morphologies of test materials were shown in Fig.11 indicating that both fractures of two kinds of joints were brittle failure by the obvious cleavage steps. Failure locations of both joints were at the position of IMCs layer shown in Fig.5a by the black dashed line. Poor connection of root interface promoted microcrack initiation and propagation initially. After analyzed the EDS results of fracture shown in Fig.11and XRD results of weld shown in Fig.8, the main phase on the fracture surface was believed to be TiCu for welding-brazing joint, but it was changed into Ti_2Cu after adjacent welding. This result is consistent with former analysis of phase transformation.

Fig.11a shows that there were lots of crystal facets and cleavage steps could be seen clearly on the fracture surface. The scale of crystal facets was small, indicating that the crack propagation was difficult and limited by the TiCu phase with high hardness. Secondary cracks could also be found and stated the high brittleness of welding-brazing joint. Fig.11b shows there were some obvious large-scale cleavage steps on the surface indicating good structural continuity of joint. The crack propagation was in the form of river pattern and there was no obvious crack. The results show that the remelting of IMCs layer and formation of Ti_2Cu phase improved the ductility of joint by reshaping the structure and the release of stress.

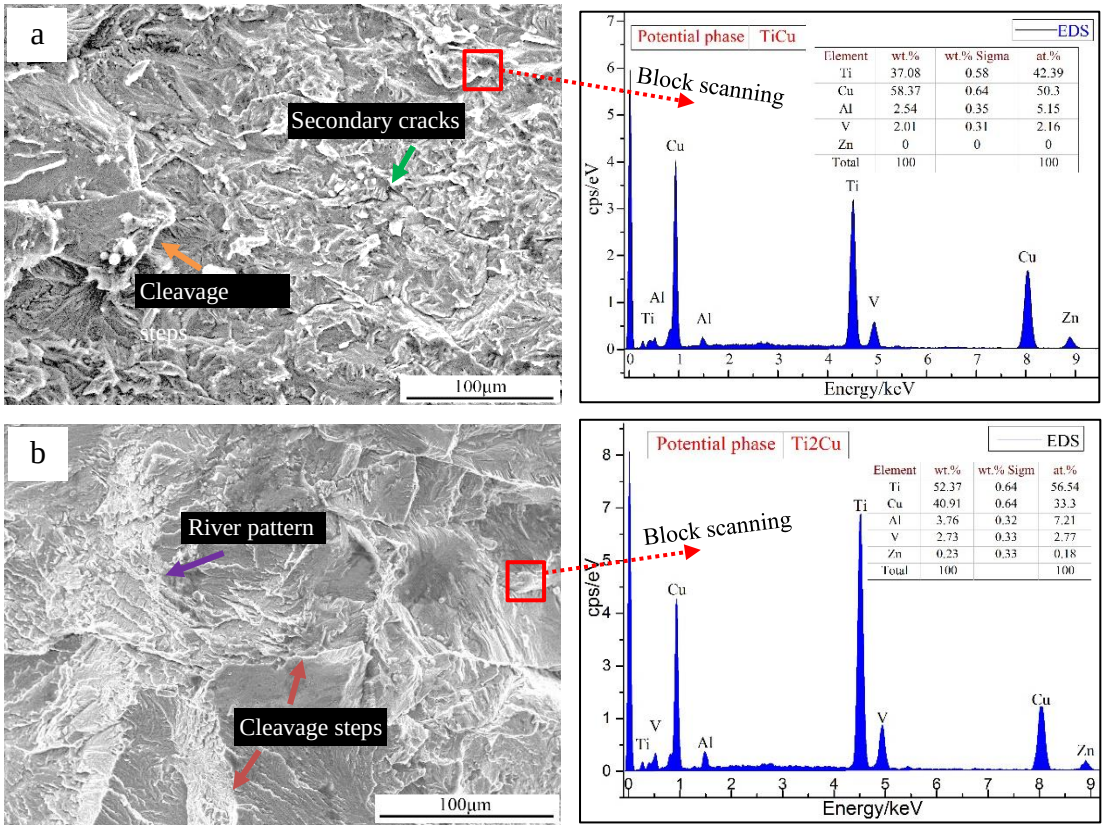

Fig.11 Fracture morphologies of joints of welding-brazing and adjacent welding: (a) joint of welding-brazing with small crystal facet characteristic and (b) joint of adjacent welding with river pattern.

4. Conclusion

1. Based on the non-centered welding process (welding-brazing process), a new innovative method called electron beam adjacent welding was proposed in this paper for the dissimilar metals welding of Ti/Cu which greatly enhanced the strength.

2. Ultimate tensile strength of Ti/Cu joints using the adjacent welding method could reach up to 89% that of copper base metal, compared to the use of traditional welding-brazing method which strength coefficient was within the limit of 70%.

3. The strengthening mechanism of adjacent welding method is due to the procedure of remelting and reverse solidification of IMCs layer, which leads to a less complex and thinner IMCs layer and then strength increased.

4. For the IMCs layer of welding-brazing joints, there were lots of compounds and low melting point eutectic including βTi+Ti_2Cu (790°C/1005°C), Ti_2Cu+TiCu (960°C), $TiCu_3$, Ti_3Cu_4, Ti_2Cu_3. In addition, TiCu with high embrittlement existed at the front of titanium substrate. These results were bad for the continuity of matrix. But after carrying out the adjacent welding, the IMCs layer had been effectively improved by the morphology reshaping, brittle phase transition from TiCu into Ti_2Cu and stress release.

5. Both fractures of welding-brazing joint and adjacent welding joint were brittle failure. There were lots of crystal facets on the facture surface of welding-brazing joint and the main phase on the surface was TiCu with high hardness, resulting in the crack propagation difficult and brittleness increase. On the surface of adjacent welding, there were some large-scale cleavage steps and crack propagation was in the form of river pattern indicating an improvement of joint ductility.

Acknowledge:

Thanks for the National Natural Science Foundations of China, Grant No. 51375243, No.51505226 and the Nature Science Foundation of Jiangsu Province, Grant No. BK20140784 supporting.

References

1. Zheng Q, Feng X, Shen Y, et al. Dissimilar friction stir welding of 6061 Al to 316 stainless steel using Zn as a filler metal[J]. Journal of Alloys & Compounds, 2016, 686:693-701.
2. Chen S, Li L, Chen Y, et al. Joining mechanism of Ti/Al dissimilar alloys during laser welding-brazing process[J]. Journal of Alloys & Compounds, 2011, 509(3):891-898.
3. Guo S, Zhou Q, Kong J, et al. Effect of beam offset on the characteristics of copper/304stainless steel electron beam welding[J]. Vacuum, 2016, 128:205-212.
4. Soysal T, Kou S, Tat D, et al. Macrosegregation in dissimilar-metal fusion welding[J]. Acta Materialia, 2016, 110:149-160.
5. Guo W, You G, Yuan G, et al. Microstructure and mechanical properties of dissimilar inertia friction welding of 7A04 aluminum alloy to AZ31 magnesium alloy[J]. Journal of Alloys & Compounds, 2017, 695: 3267-3277.
6. Cao R, Feng Z, Chen J H. Microstructures and properties of titanium-copper lap welded joints by cold metal transfer technology[J]. Materials & Design, 2014, 53: 192-201.
7. Wang T, Zhang B, Wang H, et al. kVanadium, Nickel, Copper and Silver Filler Metals[J]. Journal of Materials Engineering & Performance, 2014, 23(4):1498-1504.
8. Tomashchuk I, Sallamand P, Belyavina N, et al. Evolution of microstructures and mechanical properties during dissimilar electron beam welding of titanium alloy to stainless steel via copper interlayer[J]. Materials Science & Engineering A, 2013, 585(12):114-122.

9. Chu Q L, Zhang M, Li J H, et al. Experimental investigation of explosion-welded CP-Ti/Q345 bimetallic sheet filled with Cu/V based flux-cored wire[J]. Materials & Design, 2015, 67:606-614.
10. Kumar R, Balasubramanian M. Experimental investigation of Ti-6Al-4V titanium alloy and 304L stainless steel friction welded with copper interlayer[J]. Defence Technology, 2015, 11(1):65-75.
11. Chu Q, Zhang M, Li J, et al. Joining of CP-Ti/Q345 sheets by Cu-based filler metal and effect on interface[J]. Journal of Materials Processing Technology, 2015, 225:67-76.
12. Zakipour S, Samavatian M, Halvaee A, et al. The effect of interlayer thickness on liquid state diffusion bonding behavior of dissimilar stainless steel 316/Ti-6Al-4V system[J]. Materials Letters, 2015, 142:168-171.
13. Shiue R K, Wu S K, Chan C H. The interfacial reactions of infrared brazing Cu and Ti with two silver-based braze alloys[J]. Journal of Alloys & Compounds, 2004, 372(1-2):148-157.
14. Kumar R, Balasubramanian M. Experimental investigation of Tie6Ale4V titanium alloy and 304L stainless steel friction welded with copper interlayer[J]. Defence Technology, 2015, 11(1):65-75.
15. Meshram S D, Mohandas T, Reddy G M. Friction welding of dissimilar pure metals[J]. Journal of Materials Processing Technology, 2007, 184(1):330-337.
16. Kahraman N, Gülenç B. Microstructural and mechanical properties of Cu-Ti plates bonded through explosive welding process[J]. Journal of Materials Processing Technology, 2005, 169(1):67-71.
17. Guoyin Z U, Xiaobing L I, Zhang J, et al. Interfacial Characterization and Mechanical Property of Ti/Cu Clad Sheet Produced by Explosive Welding and Annealing[J]. Journal of Wuhan University of Technology-Mater. Sci. Ed. 2015, 30(6):1198-1203.
18. Vivek A, Liu B C, Hansen S R, et al. Accessing collision welding process window for titanium/copper welds with vaporizing foil actuators and grooved targets[J]. Journal of Materials Processing Technology, 2014, 214(214):1583-1589.
19. Aydın K, Kaya Y, Kahraman N. Experimental study of diffusion welding/bonding of titanium to copper[J]. Materials & Design, 2012, 37:356-368.
20. Yao L, Shen Y F, Li B, et al. Microstructure and properties of dissimilar materials Cu/Ti lapped joint by friction stir welding [J]. Transactions of the China Welding Institution, 2014, 35(2):109-112.
21. Węglowski M S, Błacha S, Phillips A. Electron beam Welding-Techniques and trends-Review[J]. Vacuum, 2016, 130:72-92.
22. Liu W, Chen G, Zhang B, et al. Investigation on process optimization of Cu/Ti electron beam welding[J]. Transactions of the China Welding Institution, 2008, 5: 022.
23. Chen G Q, Zhang B G, Wei L, et al. Influence of electron-beam superposition welding on intermetallic layer of Cu/Ti joint[J]. Transactions of Nonferrous Metals Society of China, 2012, 22(10):2416-2420.
24. Zhang B G, Zhao J, Xiao-Peng L I, et al. Electron beam welding of 304 stainless steel to QCr0.8 copper alloy with copper filler wire[J]. Transactions of Nonferrous Metals Society of China, 2014, 24(12):4059-4066.
25. Chen S, Huang J, Xia J, et al. Influence of processing parameters on the characteristics of stainless steel/copper laser welding[J]. Journal of Materials Processing Technology, 2015,

222:43-51.
26. Wang T, Zhang B, Feng J, et al. Effect of a copper filler metal on the microstructure and mechanical properties of electron beam welded titanium-stainless steel joint[J]. Materials Characterization, 2012, 73: 104-113.
27. Chen S, Li L, Chen Y, et al. Improving interfacial reaction nonhomogeneity during laser welding-brazing aluminum to titanium[J]. Materials & Design, 2011, 32(8): 4408-4416.
28. Dezellus O, Andrieux J, Bosselet F, et al. Transient liquid phase bonding of titanium to aluminium nitride[J]. Materials Science and Engineering: A, 2008, 495(1): 254-258.
29. Shen Q, Xiang H, Luo G, et al. Microstructure and mechanical properties of TC4/oxygen-free copper joint with silver interlayer prepared by diffusion bonding[J]. Materials Science and Engineering: A, 2014, 596: 45-51.
30. Tashi R S, Mousavi S A A A, Atabaki M M. Diffusion brazing of Ti-6Al-4V and austenitic stainless steel using silver-based interlayer[J]. Materials & Design, 2014, 54: 161-167.
31. Cao R, Feng Z, Lin Q, et al. Study on cold metal transfer welding-brazing of titanium to copper[J]. Materials & Design, 2014, 56: 165-173.
32. Bokstein B S, Vnukov V I, Golosov E V, et al. Structure and diffusion processes in laminated composites of a Cu–Ti system[J]. Russian Physics Journal, 2009, 52(8):811-815.

2017-02-20

Study on strengthening mechanism of Ti/Cu electron beam welding

Guo, S.

Elsevier

Guo S, Zhou Q, Peng Y, et al., Study on strengthening mechanism of Ti/Cu electron beam þÿwelding, Materials and Design, Volume 121, 5 May 2017, Pages 51 60. http://dx.doi.org/10.1016/j.matdes.2017.02.054